CHEMISTRY
A EUROPEAN JOURNAL

DOI: 10.1002/chem.200601194

Effects of 3d–4f Magnetic Exchange Interactions on the Dynamics of the Magnetization of Dy^{III}-M^{II}-Dy^{III} Trinuclear Clusters

Fabrice Pointillart,[a] Kevin Bernot,[a, b] Roberta Sessoli,*[a] and Dante Gatteschi[a]

Abstract: [{Dy(hfac)$_3$}$_2${Fe(bpca)$_2$}]·$CHCl_3$ ([Dy_2Fe]) and [{Dy(hfac)$_3$}$_2${Ni(bpca)$_2$}]·$CHCl_3$ ([Dy_2Ni]) (in which $hfac^- = 1,1,1,5,5,5$-hexafluoroacetylacetonate and $bpca^- =$ bis(2-pyridylcarbonyl)amine anion) were synthesized and characterized. Single-crystal X-ray diffraction shows that [Dy_2Fe] and [Dy_2Ni] are linear trinuclear complexes. Static magnetic susceptibility measurements reveal a weak ferromagnetic exchange interaction between Ni^{II} and Dy^{III} ions in [Dy_2Ni], whereas the use of the diamagnetic Fe^{II} ion leads to the absence of magnetic exchange interaction in [Dy_2Fe]. Dynamic susceptibility measurements show a thermally activated behavior with the energy barrier of 9.7 and 4.9 K for the [Dy_2Fe] and [Dy_2Ni] complexes, respectively. A surprising negative effect of the ferromagnetic exchange interaction has been found and has been attributed to the structural conformation of these trinuclear complexes.

Keywords: anisotropy · cluster compounds · lanthanides · magnetic properties · single-molecule magnets

Introduction

The design of new magnetic materials based on molecules is still one of the most important research subjects for the chemistry and physics communities. A possible way for designing a molecular material with magnetic hysteresis is the use of paramagnetic molecules with slow relaxation of the magnetization.[1] The slow dynamics of the magnetization observed in these materials known as single-molecule magnets (SMMs) is associated with the combined effects of a ground state with high-spin value (S), easy axis anisotropy ($D<0$, in which D is defined as the zero-field splitting parameter) of the cluster, and small transverse anisotropy terms. It follows an activated Arrhenius law with a characteristic energy gap Δ for reversal between up-spin and down-spin given roughly by $\Delta = |D|S^2$. To observe SMM behavior, a large J/J' ratio (in which J is the intramolecular exchange interaction and J' the intermolecular exchange interaction) is required. Slow relaxation is observed at low temperature when $|D|S^2 \gg k_B T$. The most investigated system of this type is a cluster including twelve manganese ions[2] known as Mn_{12}-acetate. Heteropolymetallic complexes have also been intensely studied[3–5] and in the continuous research to increase the blocking temperature in SMMs, highly anisotropic metal ions have been employed, like rare-earth ions. SMMs that contain both 3d and 4f have been recently investigated.[6–14] Isolated rare earth ions in high-symmetry environments, like some sandwich phthalocyanine complexes, have also revealed SMM behavior.[15,16]

The bis(2-pyridylcarbonyl)amine anion ($bpca^-$) is known for forming mononuclear complexes $[M(bpca)_2]^{n+}$ with divalent and trivalent metallic ions ($n=0$, $M^{II}=Mn^{II}$,[17] Fe^{II},[18] CuII,[19] Zn^{II}[19] and RhII;[20] $n=1$, $M^{III}=Fe^{III}$[18] and Rh^{III}[20–22]). In a next step, these complexes have allowed the obtainment of variable-dimensional materials with interesting magnetic properties: homo and heterotrimetallic complexes,[23,24] one-dimensional compounds with single chain magnet behavior,[25] and two-dimensional networks.[26] All the previous mentioned compounds show that the $bpca^-$ ligand is rather efficient in transmitting the magnetic exchange interaction between 3d ions, while little is known for 4f ions. Indeed only during the writing of this manuscript a

[a] Dr. F. Pointillart, K. Bernot, Prof. R. Sessoli, Prof. D. Gatteschi
L.A.M.M, Department of Chemistry and INSTM Research Unit
Università di Firenze, Via Della Lastruccia 3
50019 Sesto Fiorentino (FI) (Italy)
Fax: (+39) 055-457-3372
E-mail: Roberta.Sessoli@unifi.it

[b] K. Bernot
Sciences Chimiques de Rennes, UMR 6226 CNRS-INSA Rennes
Equipe "Matériaux Inorganiques: Chimie Douce et Réactivité"
INSA Rennes, 20 Avenue des Buttes de Coësmes
CS 14315, 35043 Rennes Cedex (France)

Supporting information for this article is available on the WWW under http://www.chemeurj.org/ or from the author.

work reporting the use of $bpca^-$ to form Dy^{III}-Fe^{III} dimeric species has been communicated.[12]

We report here the reaction between the precursors [M(bpca)$_2$] and [Dy(hfac)$_3$]·2H$_2$O ($hfac^- = 1,1,1,5,5,5$-hexafluoroacetylacetonate) that leads to the 3d–4f trinuclear complexes [{Dy(hfac)$_3$}$_2${M(bpca)$_2$}]·CHCl$_3$ (M = Fe^{II} and Ni^{II}). Both complexes have been characterized by X-ray diffraction. The use of the paramagnetic [Ni(bpca)$_2$] unit permits an exchange interaction between the two external anisotropic [Dy(hfac)$_3$] centers, while by using a diamagnetic central unit like [Fe(bpca)$_2$], it is possible to isolate magnetically the rare earth ions and thus to highlight the effect of weak magnetic exchange interactions on the static and dynamic magnetic susceptibility of these trinuclear complexes.

Results and Discussion

Synthesis: It is known that the donor complexes [M^{II}(bpca)$_2$] can give polynuclear compounds by using their four carbonyl groups[23–26] to bridge other metal ions. The synthesis of transition-metal derivatives were made by using $CHCl_3$ as solvent at room temperature, while with lanthanide ions we choose to perform the reaction at 50–60 °C.

The lanthanide ions have a higher affinity for the water molecules than the transition metal ions. Hence a dehydratation of the [Dy(hfac)$_3$]·2H$_2$O precursors was needed to react with the complexes [M(bpca)$_2$] (M = Fe^{II} and Ni^{II}). The dehydratation is favored by giving thermal energy to the system.

Table 1. Crystallographic data for [{Dy(hfac)$_3$}$_2${Fe(bpca)$_2$}]·CHCl$_3$, ([Dy$_2$Fe]) and [{Dy(hfac)$_3$}$_2${Ni(bpca)$_2$}]·CHCl$_3$, ([Dy$_2$Ni]).

	[Dy$_2$Fe]	[Dy$_2$Ni]
formula	$C_{55}H_{23}N_6O_{16}Cl_3F_{36}Dy_2Fe$	$C_{55}H_{23}N_6O_{16}Cl_3F_{36}Dy_2Ni$
M_r [g mol^{-1}]	2194.4	2197.2
crystal system	monoclinic	monoclinic
space group	$P2_1/b$	$P2_1/b$
a [Å]	21.250(2)	21.141(5)
b [Å]	17.161(2)	17.479(5)
c [Å]	21.403(3)	21.326(5)
β [°]	111.114(12)	110.319(5)
V [Å^3]	7281.29(11)	7390.23(9)
Z	4	4
T [K]	150(2)	150(2)
2θ range [°]	7.88–44.92	8.10–7.64
ρ_{calcd} [Mg m^{-3}]	1.893	1.975
μ [mm^{-1}]	2.385	2.519
reflns collected	25 714	31 081
independent reflns	9355	11 111
observed reflns [$F_o > 4\sigma(F_o)$]	3665	6323
parameters	1072	1072
R_1/wR_2	0.0786/0.1741	0.0526/0.1109

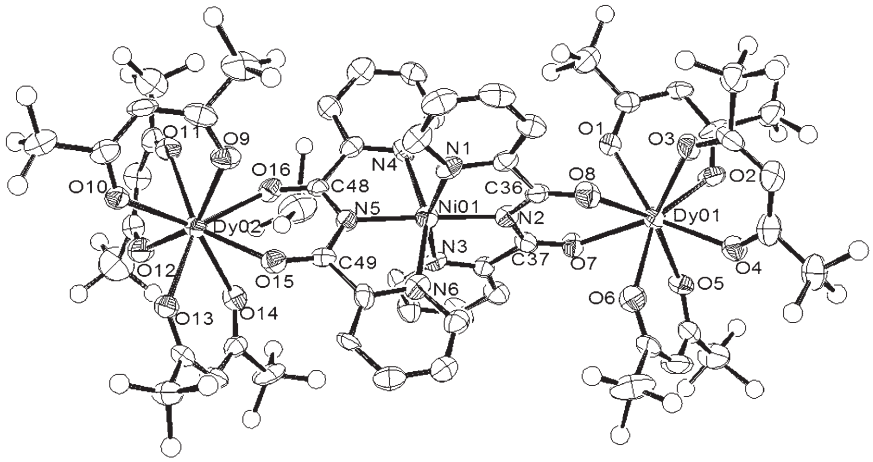

Figure 1. ORTEP[27] view of [Dy$_2$Ni] with thermal ellipsoids at 50% probability. Hydrogen atoms and thermal ellipsoids for fluorine atoms are omitted for clarity.

X-ray crystallography: Compounds [Dy$_2$Fe] and [Dy$_2$Ni] crystallize in the $P2_1/b$ space group (Table 1). The asymmetric unit is shown in Figure 1 for [Dy$_2$Ni] and in Figure S1 of the Supporting Information for [Dy$_2$Fe]. It is composed of one central M^{II} ion surrounded by two $bpca^-$ ligands, linked by pyridine and amine groups, two Dy^{III} ions surrounded by three $hfac^-$ ligands and the two carbonyl groups of the $bpca^-$ ligands, and one crystallization chloroform molecule. Selected bond lengths and angles are given in the Tables 2 and 3 for both compounds.

The two derivatives [Dy$_2$Fe] and [Dy$_2$Ni] have a very similar crystallographic structure. The main difference is found in the position of the chloroform molecule. Actually, in [Dy$_2$Fe] the distances between the carbon atom of the chloroform molecule (C55) and the nearest metallic ions are 4.487 (Dy02–C55) and 8.352 Å (Fe01–C55), whereas in [Dy$_2$Ni] they are 6.561 and 6.743 Å.

In both compounds a central [M(bpca)$_2$] (M = Fe^{II}, Ni^{II}) unit is linked to two terminal [Dy(hfac)$_3$] units and the angle formed by the two N_{amide} atoms and the central metallic ion is close to linearity with values of 178.2(6)° and 178.2(3)° in [Dy$_2$Fe] and [Dy$_2$Ni], respectively (Table 3). This leads to a linear structure of the trinuclear clusters in which the two terminal Dy^{III} ions are located roughly at the same distance of the central M^{II} ion (5.65 Å in [Dy$_2$Fe] and 5.73 Å in [Dy$_2$Ni]) while the Dy–Dy distances are 11.316 and 11.464 Å, respectively.

The central metal ion is linked to six nitrogen atoms localized in a range 1.913–1.969 Å for central ion M = Fe^{II} and 2.004–2.111 Å for M = Ni^{II}. In the latter case the antibonding e_g orbitals are partially filled leading to a slight increase of the ionic radius. The mean length of the two M^{II}–N_{amide} bonds (1.923 Å for [Dy$_2$Fe] and 2.007 Å for [Dy$_2$Ni]) are

Table 2. Selected bond lengths [Å] for [Dy_2Fe] and [Dy_2Ni].

[Dy_2Fe]		[Dy_2Ni]	
Fe01–N_{amide}2	1.913(14)	Ni01–N_{amide}2	2.009(7)
Fe01–N_{amide}5	1.932(12)	Ni01–N_{amide}5	2.004(7)
Fe01–N_{py}1	1.920(14)	Ni01–N_{py}1	2.096(7)
Fe01–N_{py}3	1.950(15)	Ni01–N_{py}3	2.093(7)
Fe01–N_{py}4	1.969(13)	Ni01–N_{py}4	2.109(7)
Fe01–N_{py}6	1.941(14)	Ni01–N_{py}6	2.111(8)
Dy01–O1	2.412(12)	Dy01–O1	2.368(6)
Dy01–O2	2.302(12)	Dy01–O2	2.331(7)
Dy01–O3	2.315(11)	Dy01–O3	2.336(6)
Dy01–O4	2.360(12)	Dy01–O4	2.328(6)
Dy01–O5	2.321(11)	Dy01–O5	2.329(6)
Dy01–O6	2.366(11)	Dy01–O6	2.338(6)
Dy01–O7	2.340(12)	Dy01–O7	2.360(6)
Dy01–O8	2.444(12)	Dy01–O8	2.354(6)
Dy02–O9	2.376(13)	Dy02–O9	2.344(6)
Dy02–O10	2.345(11)	Dy02–O10	2.354(6)
Dy02–O11	2.347(12)	Dy02–O11	2.331(6)
Dy02–O12	2.340(11)	Dy02–O12	2.300(6)
Dy02–O13	2.308(14)	Dy02–O13	2.309(6)
Dy02–O14	2.346(13)	Dy02–O14	2.390(6)
Dy02–O15	2.335(10)	Dy02–O15	2.389(6)
Dy02–O16	2.381(11)	Dy02–O16	2.343(6)
O8–C36	1.232(19)	O8–C36	1.226(10)
O7–C37	1.220(20)	O7–C37	1.237(10)
O16–C48	1.250(20)	O16–C48	1.230(10)
O15–C49	1.234(18)	O15–C49	1.237(10)
Dy01–Dy02	11.316(26)	Dy01–Dy02	11.464(27)
Dy01–Fe1	5.647(14)	Dy01–Ni01	5.731(14)
Dy02–Fe1	5.648(14)	Dy02–Ni01	5.737(13)

Table 3. Selected angles [°] for [Dy_2Fe] and [Dy_2Ni].

[Dy_2Fe]		[Dy_2Ni]	
N_{amide}2-Fe01-N_{amide}5	178.2(6)	N_{amide}2-Ni01-N_{amide}5	178.2(3)
N_{py}1-Fe01-N_{py}3	163.6(6)	N_{py}1-Ni01-N_{py}3	158.9(3)
N_{py}4-Fe01-N_{py}6	163.1(6)	N_{py}4-Ni01-N_{py}6	157.2(3)
Dy01-Fe01-Dy02	177.6(5)	Dy01-Ni01-Dy02	177.2(2)

shorter than those of the four M^{II}–N_{py} bonds (1.945 Å for [Dy_2Fe] and 2.105 Å for [Dy_2Ni]), because the negative charge on the $bpca^-$ ligand is principally localized on the amide nitrogen atoms. The angles formed by the N_{py} atoms and the central metal ions have values significantly different from 180° (Table 3). Thus the coordination polyhedrons around the central metallic ion can be described by a distorted slightly compressed octahedron.

In both compounds the Dy^{III} ions are linked to eight oxygen atoms localized in a range 2.300–2.444 Å. The coordination polyhedron of the Dy^{III} lanthanides has been described as a distorted dodecahedron, the distortion is mainly due to the existence of two Dy–O bonds longer than the others. These two long Dy–O bonds can be attributed to a slight steric hindrance between the $bpca^-$ ligand and the nearest $hfac^-$ ligand.

Figure 2 shows the packing of the trinuclear complexes in the crystal and the intramolecular (11.31 Å) and intermolecular (9.84 Å) shortest distances between the Dy^{III} ions for [Dy_2Fe]. These distances are 11.46 Å and 9.53 Å in the case of [Dy_2Ni]. No π-stacking or short contacts occur between the complexes and the trinuclear units are well isolated one from each other.

Static magnetic susceptibility: The thermal dependences of $\chi_M T$ are shown in the Figure 3 for [Dy_2Fe] and [Dy_2Ni]. The $\chi_M T$ product takes a quasi-constant value equal to 28.5 $cm^3 K mol^{-1}$ for [Dy_2Fe] in the temperature range 300–125 K, while the $\chi_M T$ product of [Dy_2Ni] shows a slight increase on lowering the temperature from 29.8 $cm^3 K mol^{-1}$ at 300 K to 30.2 $cm^3 K mol^{-1}$ at 125 K. Below 125 K, the $\chi_M T$ product of both trinuclear complexes decreases continuously down to values of 23.3 and 19.0 $cm^3 K mol^{-1}$ at 2 K, respectively, for [Dy_2Ni] and [Dy_2Fe]. The inset of the Figure 3 shows the plot of the thermal dependence of the difference $\Delta\chi_M T$ (with $\Delta\chi_M T = \chi_M T_{[Dy_2Ni]} - \chi_M T_{[Dy_2Fe]}$). The $\Delta\chi_M T$ product increases slowly from 1.35 to 2 $cm^3 K mol^{-1}$ in the range of temperature 300–50 K. Below 15 K the $\Delta\chi_M T$ product increases faster to reach the value of 4.28 $cm^3 K mol^{-1}$ at 2 K.

In the trinuclear complex [Dy_2Fe], the central Fe^{II} ion has an electronic configuration d^6 low spin ($S=0$) known for both the free and coordinated [$Fe(bpca)_2$] unit.[18,23] Consequently the experimental value is close to the expected one for two magnetically independent Dy^{III} ions (28.34 $cm^3 K mol^{-1}$). The observed room temperature value

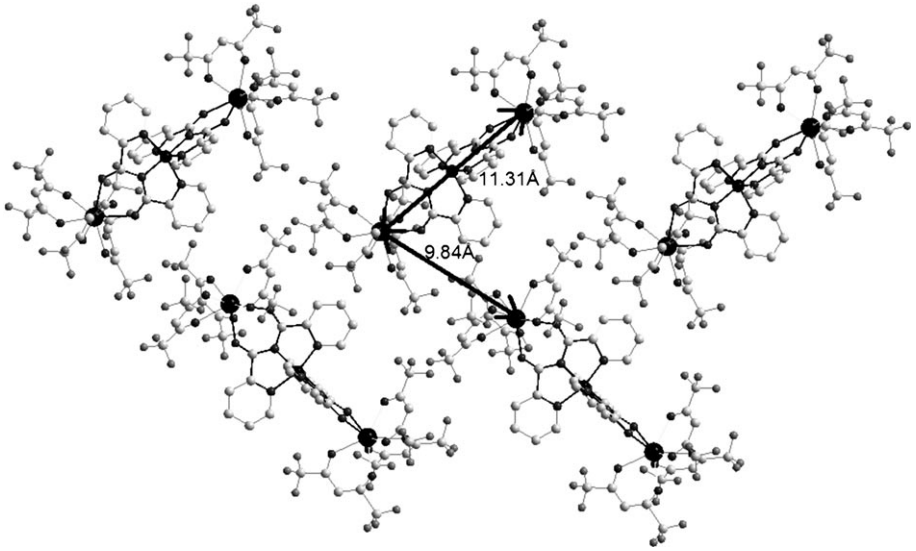

Figure 2. View of the packing crystal of [Dy_2Fe] showing the arrangement of the trinuclear complexes and the intramolecular (11.31 Å) and intermolecular (9.84 Å) shortest distances between the Dy^{III} ions.

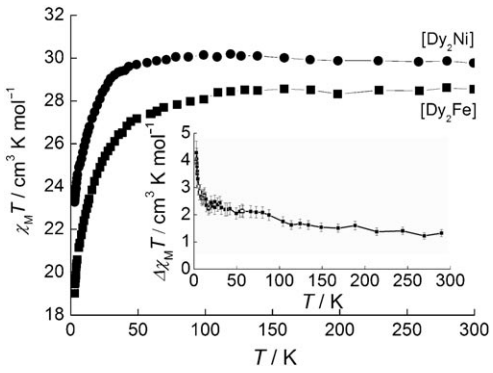

Figure 3. Temperature dependence of the product $\chi_M T$ for [Dy_2Ni] (open circles) and [Dy_2Fe] (filled squares). In the inset, a plot of the difference $\Delta\chi_M T$ (with $\Delta\chi_M T = \chi_M T_{[Dy_2Ni]} - \chi_M T_{[Dy_2Fe]}$) as a function of the temperature.

for the compound [Dy_2Ni] is in agreement with the theoretical one (29.42 $cm^3 K mol^{-1}$) for three uncoupled metallic ions (two Dy^{III} ions and one Ni^{II} $S=1$, $g=2.08$). The ground state for a Dy^{III} ion is $^6H_{15/2}$ characterized by $g_J=4/3$.[28] The first excited state ($^6H_{13/2}$) is separated by more than 1500 cm^{-1} from the ground state.[29] The latter is split in Stark sublevels under the influence of a crystal field.[30] The crystal-field effects are of the order of 100 cm^{-1} for lanthanides. When the temperature decreases, the depopulation of these sub-levels leads to a deviation from the Curie law observed by a variation of the $\chi_M T$ product even in the absence of any exchange interaction. Eventually, at low temperature only the ground Kramers doublet is populated and the magnetic properties are modeled by using an effective spin $S_{eff}=1/2$ with a very anisotropic g_{eff} value. Below 125 K, the decrease of the $\chi_M T$ product for [Dy_2Fe] is therefore only attributed to the depopulation of the Stark sublevels of the two Dy^{III} ions. The temperature dependence of $\Delta\chi_M T$ (inset of Figure 3), which can be considered to be free from the influence of the crystal field effects of the terminal Dy^{III} ions, clearly shows that a weak Dy–Ni ferromagnetic exchange interaction mediated by the $bpca^-$ ligand is active.

Dynamic magnetic susceptibility: In-phase and out-of-phase components of the ac-susceptibility were recorded using 12 logarithmic spaced frequencies in the range 100–25 000 Hz between 1.55 and 3.5 K on both complexes. In the absence of external field the out-of-phase signal observed for [Dy_2Fe] is very weak with a low ratio χ'/χ'' and almost undetectable for [Dy_2Ni], as indeed observed in reference [12] for a $Dy^{III}Fe^{III}$ binuclear complex.

Recent results on phthalocyaninate derivatives of lanthanide ions[15,16] have shown that such behavior can be due to fast zero-field tunneling of the magnetization that can be suppressed by applying a static field. In these conditions useful information on the dynamics of the magnetization in the thermally activated regime can anyhow be extracted. We have therefore recorded χ_{ac} versus frequency for several applied static fields and some selected data are shown in Figure 4. As predicted, a strong field dependence of χ'' is visible on both complexes. In both cases the maximum in χ'' is shifted to the lowest frequency for an applied field around 1 kOe and shifts again to higher frequencies at stronger static fields. A field of 1 kOe was therefore selected to investigate the temperature dependence of the dynamic susceptibility.

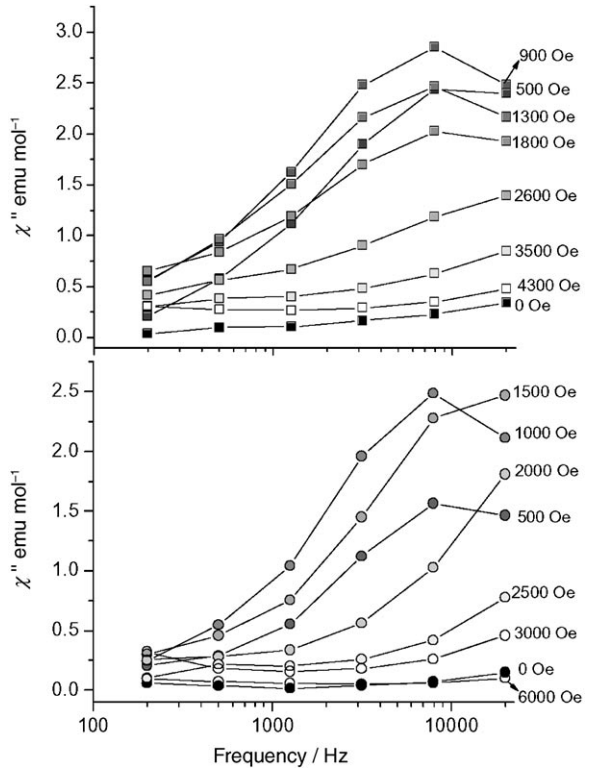

Figure 4. Frequency dependence of the imaginary χ'' component of the ac-susceptibility for [Dy_2Fe] (top, square) and [Dy_2Ni] (bottom, circle) measured for increasing strength of the dc field (from black to white) at $T=1.8$ K.

The temperature dependence of χ' and χ'' versus frequency for [Dy_2Fe] and for [Dy_2Ni] are shown in Figure 5, while the same data plotted versus temperature are given in the Supporting Information as Figures S2 and S3, respectively. The application of the field switches from a noisy and weak χ'' signal to a quite strong out-of-phase contribution to the dynamic susceptibility, with values of χ' and χ'' of the same order of magnitude. This is characteristic of SMMs presenting a narrow distribution of the relaxation times.[1]

To better characterize the distribution we have plotted the normalized χ'' versus χ' in the Argand plot. The extracted curves, as depicted in Figure 6 for $T=1.6$ K, could be fitted with an extended Debye model by using Equation (1)[31] in which χ_T is the isothermal susceptibility, χ_S the adiabatic susceptibility, ω is the angular frequency of the ac field and τ is the relaxation time of the system at the temperature at which the fit is performed. The parameter α

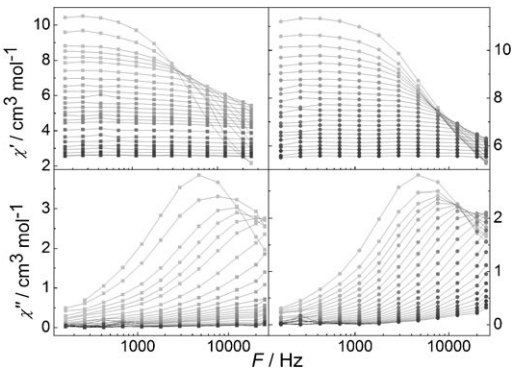

Figure 5. Frequency dependence of the real χ' (top) and imaginary χ'' (bottom) components of the ac-susceptibility for [Dy_2Fe] (left) and [Dy_2Ni] (right) measured in 1 kOe static applied field and in 162 to 25000 Hz frequency range. The temperatures used span from 1.55 K (light grey) to 4 K (dark grey). Lines are guides to the eyes.

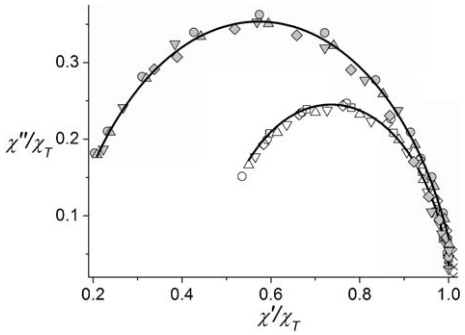

Figure 6. Argand diagram taken for [Dy_2Fe] (filled symbols) and for [Dy_2Ni] (open symbols) in the temperature range 1.6–2.0 K. The lines represent the best-fit calculated values for $T=1.6$ K with an extended Debye model providing: $\alpha=0.12\pm0.03$ and $R=0.996$ for [Dy_2Fe], $\alpha=0.03\pm0.01$ and $R=0.995$ for [Dy_2Ni].

takes into account the width of the distribution, being zero for an infinitely narrow distribution.

$$\chi(\omega)=\chi_S+\frac{\chi_T-\chi_S}{1+(i\omega\tau)^{1-\alpha}} \quad (1)$$

The fitting of the experimental data at $T=1.6$ K has provided $\alpha=0.12\pm0.03$ for [Dy_2Fe] and $\alpha=0.03\pm0.01$ for [Dy_2Ni] with no significant variations up to 2.0 K. These small values are fully compatible with SMM behavior. Interestingly the two compounds have very different χ_S values, almost zero for [Dy_2Fe] and around $0.5\chi_T$ for [Dy_2Ni]. In this last case a significant fraction of the magnetization appears to relax much faster, as it will be discussed later.

From the frequency at which the maximum in χ'' occurs we have extracted the characteristic time constant as $\tau=\omega^{-1}$. In SMMs the temperature dependence of the relaxation time is well described by the Arrhenius law [Eq. (2)], with $\Delta=|D|S^2$ for integer spin.[1]

$$\tau=\tau_0 e^{\Delta/k_BT} \quad (2)$$

This behavior results from a multiphonon process involving all the levels of the double well potential originated by the magnetic anisotropy $H_{an}=DS_z^2$, with a large value of S. Such a behavior was justified by extending the two-phonon Orbach process.[32] It is, in principle, not expected for the present compounds, in particular in the case of [Dy_2Fe] in which each Dy center should behave like an isolated lanthanide ion. The field dependence of the relaxation time, showing a non-monotonous behavior, suggests that the relaxation does not occur through a direct mechanism involving the $|+\rangle$ and $|-\rangle$ components of the ground doublet of the $J=15/2$ multiplet. In this last case a field dependence $\tau\propto H^{-n}$ (with n between 2 and 5) would be expected.[33] In the investigated temperature range the relaxation process is expected to be dominated by a classical two-phonon (Orbach) mechanism, in which the system first is excited to an intermediated state by adsorbing a phonon and then relaxes to the final state emitting a phonon, the energy of which can be equal to, or slightly different from, the adsorbed one.[33] This process results therefore to be thermally activated and gives rise to the exponential dependence on the temperature of Equation (2). The parameter Δ represents the separation between the ground state and the excited ones involved in the relaxation process. For the lanthanides this separation is related to low-symmetry components of the crystal field and therefore is somehow related to the magnetic anisotropy. The pre-exponential factor (in seconds) for lanthanide ions have been estimated in the order of Δ^{-3} multiplied by a factor in the range of 10^{-3}–10^{-5}.[33]

The temperature dependence of the relaxation time, reported in Figure 7 for both compounds in the Arrhenius plot shows a linear behavior typical of the Orbach mechanism. The results of the linear analysis, reported in Table 4, highlight significant differences between the two compounds, even if the accuracy of the parameters is limited by the narrow range of investigable temperatures. In particular [Dy_2Ni] has an almost halved activation energy relative to [Dy_2Fe], despite the ferromagnetic interaction with the central Ni^{II} ion.

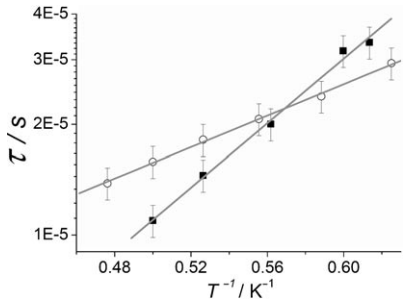

Figure 7. Arrhenius plot extracted for the [Dy_2Fe] (filled square) and [Dy_2Ni] (open circles) trinuclear complexes. Linear regression performed on the data gave the parameters reported in Table 4 with $R=0.9997$ for [Dy_2Fe] and $R=0.9989$ for [Dy_2Ni].

Table 4. Main magnetic data extracted from the dynamic properties of the trinuclear compounds.

	τ_0 [s]	Δ [K]	α
[Dy_2Fe]	$8.7(\pm0.2)\times10^{-8}$	9.7(±0.4)	0.12 ± 0.03
[Dy_2Ni]	$1.3(\pm0.2)\times10^{-6}$	4.9(±0.3)	0.03 ± 0.01

Recently, many compounds composed of transition-metal ions and the [$Dy(hfac)_3$] unit have shown a SMM behavior.[6,7,9,34] The general idea of combining the magnetic anisotropy of the lanthanide with the magnetic interaction involving transition metal ions in order to build a larger magnetic moment for the molecule appears not to work in the present case.

In our investigation the inclusion of ferromagnetic exchange interaction indeed halves the energy barrier, while the crystal field splitting of the Dy^{III} centers is expected to remain unchanged, given that the compounds are practically isostructural.

The structure of these trinuclear compounds and the strong anisotropy of the Dy^{III} ion could explain the trend observed for Δ. In fact, the two planes described by the two O-C-N_{amide}-C-O fragments around the transition-metal ions form an angle of about 80°. The rigidity of the $bpca^-$ ligand forces the Dy^{III} coordination polyhedrons to be almost perpendicular to each other. If the Ising type magnetic anisotropy of the Dy^{III} ions dominates[35] and the easy axis of each Dy^{III} ion is not accidentally oriented along the Dy–Ni direction, the structural conformation of the trinuclear compounds leads to a strong reduction of the magnetic anisotropy of the two Dy^{III} ions of the complex. It is interesting to note that the same orthogonal orientation of the $bpca^-$ ligands, which here reduces the energy barrier, has been shown to be favorable if magnetic centers with easy plane anisotropy are coupled.[25]

It is also interesting to note that the opposite trend is observed for the pre-exponential factor (τ_0) of [Dy_2Ni]; it is about 20 times longer than that of [Dy_2Fe], leading to a slower relaxation of the former in the high temperature regime (see Figure 7). The pre-exponential factor is strongly affected by the speed of sound, but also related to the phonon modulation of the magnetic anisotropy. It is therefore not surprising that in the two almost isostructural compounds investigated here, the reduction of the magnetic anisotropy is accompanied by its reduced dependence on the lattice vibrations with the consequent increase of τ_0. A similar trend has been indeed observed for SMMs[36] and is in agreement with the Δ^{-3} dependence predicted for the Orbach mechanism.[33]

In an alternative picture the reduction of the energy barrier could be due to the presence of low-lying states originated by the exchange interaction. This hypothesis is, however, in contrast with the result very recently obtained by Yamashita et al.[12] In their dinuclear compound, formed by one $[Fe(bpca)_2]^+$ unit and one Dy^{III} ion antiferromagnetically coupled, the observed energy barrier is $\Delta = 13.8$ K. Even if they have not provided any experimental value for the energy barrier of the isolated Dy^{III} ion, the observed Δ value is not comparable with the exchange splitting that they estimate of the order of 0.1 K. In their case the coordination of only one of the two O-C-N_{amide}-C-O units prevents a geometrical reduction of the Ising anisotropy.

More evidence for the key-role played by the paramagnetic Ni^{II} ion in mediating the magnetic anisotropy of the two non-collinear terminal Dy^{III} ions comes from the Argand plot of [Dy_2Ni], which shows a large χ_s value, which is practically zero in [Dy_2Fe]. The fraction of the magnetization that relaxes much faster is much larger than that of an isolated Ni^{II} ion and is therefore intrinsic of the trimeric species. It could be associated to the transverse component of the magnetization of a system exhibiting easy axis anisotropy. This component is, however, very small for isolated Ising type ions, as indeed observed for [Dy_2Fe]. In contrast, it can become significantly large, but still fast-relaxing, if the easy axes of the magnetization of coupled systems are not collinear.[37] A single-crystal study is necessary to shed more light on this observation.

Conclusion

We have reported here the structural and magnetic properties of two isostructural [Dy_2Fe] and [Dy_2Ni] compounds. Thanks to the comparison of the magnetic behavior in the presence of a paramagnetic or a diamagnetic central ion we have shown that the $bpca^-$ ligand can transmit a ferromagnetic exchange interaction between 3d and 4f metal ions. The same approach has provided interesting information on the role played by the 3d metal ion in the dynamics of 3d–4f single-molecule magnets.

The dynamics of the magnetization has been investigated under a relatively weak external field to suppress fast tunneling, often observed in zero field. Surprisingly the energy barrier for the reversal of the magnetization is strongly reduced when the ferromagnetic interaction is active. The orthogonal arrangement of the Dy^{III} coordination polyhedrons, due to the coordination of the two $bpca^-$ ligands, seems to be responsible for this observation. The structural conformation of these compounds can lead to the cancellation of a significant fraction of the Ising anisotropy of the two terminal Dy^{III} ions.

It is therefore evident that the inclusion of exchange interactions mediated by transition-metal ions is not sufficient to build SMMs that are mainly based on lanthanide ions. An appropriate choice of the ligand in order to control the orientation of the anisotropy axes is crucial for lanthanides. Moreover, the procedure employed here, that is, the parallel investigation of the dynamic properties of the isolated metal ions in the same coordination environment, appears as an unavoidable step in order to correctly evaluate the success of a rational design of lanthanide-based SMMs.

Experimental Section

Synthesis: Hbpca ligand,[23] $[Ni(bpca)_2]$,[23] $[Fe(bpca)_2]$[18] and $[Dy(hfac)_3]\cdot 2H_2O$[27] complexes were synthesized according to literature methods. All other reagents were purchased from Aldrich and used as received.

Synthesis of trinuclear complexes $[Dy_2Ni]$ and $[Dy_2Fe]$

Complex $[Dy_2Ni]$: A solution $[Dy(hfac)_3]\cdot 2H_2O$ (48.9 mg, 0.06 mmol) in $CHCl_3$ (5 mL) was added to a boiling solution of $[Ni(bpca)_2]$ (15 mg, 0.029 mmol) in $CHCl_3$ (10 mL) . The resulting mixture was stirred for 20 min at 50 °C. Slow evaporation of the solution at room temperature gave orange single crystals, which were filtered and dried in air. Yield: 54.8 mg (86 %); elemental analysis calcd (%) for $Dy_2NiC_{55}H_{23}N_6O_{16}F_{36}Cl_3$: C 30.04, H 1.05, N 3.82; found: C 30.24, H 1.17, N 3.80.

Complex $[Dy_2Fe]$: Small black single crystals suitable for X-ray diffraction were obtained by using a similar procedure to that described for $[Dy_2Ni]$, but with $[Fe(bpca)_2]$ (14.7 mg, 0.029 mmol) in place of $[Ni(bpca)_2]$. Yield: 50.3 mg (79 %); elemental analysis calcd (%) for $Dy_2FeC_{55}H_{23}N_6O_{16}F_{36}Cl_3$: C 30.08, H 1.05, N 3.83; found: C 30.29, H 1.13, N 3.84.

Physical measurements: X-ray data for both compounds were collected at low temperature with an Oxford Diffraction Xcalibur3 diffractometer by using $Mo_{K\alpha}$ radiation ($\lambda = 0.71073$ Å). Data reduction was accomplished using CRYSALIS.RED p171.29.2.[38] Absorption correction was performed by using both ABSGRAB and ABSPACK software included in the Crysalis package. The ABSGRAB correction allows for a determination of μ parameter (reported in Table 1). The structure was solved by direct methods, developed by successive difference Fourier syntheses, and refined by full-matrix least-squares on all F^2 data using SHELXL 97.[39] Hydrogen atoms were included in calculated positions and allowed to ride on their parent atoms. CCDC-615957 and CCDC-615958 contains the supplementary crystallographic data for this paper. These data can be obtained free of charge from The Cambridge Crystallographic Data Centre via www.ccdc.cam.ac.uk/data_request/cif.

The dc-magnetic susceptibility measurements were performed on solid polycrystalline samples with a Cryogenic S600 SQUID magnetometer between 2 and 300 K in applied magnetic field of 0.01 T for temperatures of 2–65 K, 0.1 T for temperatures of 65–250 K and 1 T for temperatures of 250–300 K. These measurements were all corrected for the diamagnetic contribution as calculated with Pascal's constants. The ac-magnetic susceptibility measurements were performed using a homemade probe operating in the range 100–25 000 Hz.[40] All measurements were performed on pellets in order to avoid orientation on these very anisotropic materials.

Acknowledgements

We acknowledge the financial support from Italian MURST (FIRB and PRIN grants), from the EC through the Human Potential Program RTN-QUELMOLNA (MRTN-CT-2003-504880), from the NE-MAGMANET (NMP3-CT-2005-515767). F.P. thanks German DFG (SPP1137) for his post-doctoral fellowship. S. Ciattini is acknowledged for his help on crystallographic measurements.

[1] D. Gatteschi, R. Sessoli, J. Villain, *Molecular Nanomagnets*, Oxford University Press, Oxford, **2006**.
[2] a) T. Lis, *Acta Crystallogr. Sect. B* **1980**, *36*, 2042; b) R. Sessoli, H. L. Tsai, A. R. Schake, S. Wang, J. B. Vincent, K. Folting, D. Gatteschi, G. Christou, D. N. Hendrickson, *J. Am. Chem. Soc.* **1993**, *115*, 1804; c) G. Christou, D. Gatteschi, D. N. Hendrickson, R. Sessoli, *MRS Bull.* **2000**, *25*, 66.
[3] a) T. Kido, S. Nagasato, Y. Sunatsuki, N. Matsumoto, *Chem. Commun.* **2000**, 2113; b) T. Kido, Y. Ikuta, Y. Sunatsuki, Y. Ogawa, N. Matsumoto, N. Re, *Inorg. Chem.* **2003**, *42*, 398.
[4] J.-P. Costes, F. Dahan, A. Dupuis, J.-P. Laurent, *Chem. Eur. J.* **1998**, *4*, 1616.
[5] R. Gheorghe, P. Cucos, M. Andruh, J.-P. Costes, B. Donnadieu S. Shova, *Chem. Eur. J.* **2006**, *12*, 187.
[6] F. Mori, T. Ishida, T. Nogani, *Polyhedron* **2005**, *24*, 2588.
[7] F. Mori, T. Nyui, T. Ishida, T. Nogami, K-Y. Choi, H. Nojiri, *J. Am. Chem. Soc.* **2006**, *128*, 1440.
[8] A. Mishra, W. Wernsdorfer, K. A. Abboud, G. Christou, *J. Am. Chem. Soc.* **2004**, *126*, 15 648.
[9] S. Osa, T. Kido, N. Matsumoto, N. Re. , A. Pochaba, J. Mrozinski, *J. Am. Chem. Soc.* **2004**, *126*, 420.
[10] C. M. Zaleski, F. C. Depperman, J. W. Kampf, M. L. Kirk, V. L. Pecoraro, *Angew. Chem.* **2004**, *116*, 4002; *Angew. Chem. Int. Ed.* **2004**, *43*, 3912.
[11] M. Murugesu, A. Mishra, W. Wernsdorfer, K. A. Abboud G. Christou, *Polyhedron* **2006**, *25*, 613.
[12] M. Ferbinteanu, T. Kajiwara, K-Y. Choi, H. Nojiri, A. Nakamoto, N. Kojima, F. Cimpoesu, Y. Fujimura, S. Takaishi, M. Yamashita, *J. Am. Chem. Soc.* **2006**, *128*, 9008.
[13] a) J.-P. Costes, J.-M. Clemente-Juan, F. Dahan, J. Milon, *Inorg. Chem.* **2004**, *43*, 8200; b) .J.-P. Costes, F. Dahan, W. Wernsdorfer, *Inorg. Chem.* **2006**, *45*, 5.
[14] C. Aronica, G. Pilet, G. Chastanet, W. Wernsdorfer, J.-F. Jacquot, D. Luneau, *Angew. Chem.* **2006**, *118*, 28, 4775; *Angew. Chem. Int. Ed.* **2006**, *45*, 4659.
[15] N. Ishikawa, M. Sugita, W. Wernsdorfer, *J. Am. Chem. Soc.* **2005**, *127*, 3650.
[16] N. Ishikawa, M. Sugita, W. Wernsdorfer, *Angew. Chem.* **2005**, *117*, 2991; *Angew. Chem. Int. Ed.* **2005**, *44*, 2931.
[17] D. Marcos, J.-V. Folgado, D. Beltran-Porter, M. T. Do Prado-Gambardella, S. H. Pulcinelli, R. H. De Almeida-Santos, *Polyhedron* **1990**, *9*, 2699.
[18] S. Wocadlo, W. Massa, J-V. Folgado, *Inorg. Chim. Acta* **1993**, 207, 199.
[19] D. Marcos, R. Martinez-Manez, J-V. Folgado, A. Beltran-Porter, D. Beltran-Porter, A. Fuertes, *Inorg. Chim. Acta* **1989**, *159*, 11.
[20] P. Paul, B. Tyagi, A. K. Bilakhiya, M. M. Bhadbhade, E. Suresh, *J. Chem. Soc. Dalton Trans.* **1999**, 2009.
[21] P. Paul, B. Tyagi, A. K. Bilakhiya, M. M. Bhadbhade, E. Suresh, G. Ramachandraiah, *Inorg. Chem.* **1998**, *37*, 5733.
[22] P. Paul, B. Tyagi, A. K. Bilakhiya, M. M. Bhadbhade, E. Suresh, *J. Chem. Soc. Dalton Trans.* **1997**, 2273.
[23] A. Kamiyama, T. Noguchi, T. Kajiwara, T. Ito, *Inorg. Chem.* **2002**, *41*, 507.
[24] T. Kajiwara, R. Sensuri, T. Noguchi, A. Kamiyama, T. Ito, *Inorg. Chim. Acta* **2002**, *337*, 299.
[25] T. Kajiwara, M. Nakano, Y. Kaneko, S. Takaishi, T. Ito, M. Yamashita, A. I. Kamiyama, H. Nojiri, Y. Ono, N. Kojima, *J. Am. Chem. Soc.* **2005**, *127*, 10 150.
[26] A. Kamiyama, T. Noguchi, T. Kajiwara, T. Ito, *Angew. Chem.* **2000**, *112*, 3260; *Angew. Chem. Int. Ed.* **2000**, *39*, 3130.
[27] C. K. Johnson, ORTEP, Report ORNL-5138, Oak Ridge National Laboratory, Oak Ridge, TN, **1976**.
[28] C. Benelli, D. Gatteschi, *Chem. Rev.* **2002**, *102*, 2369.
[29] O. Kahn, *Molecular Magnetism*, VCH, Weinhem, **1993**.
[30] J. P. Sutter, M. L. Kahn, *Magnetism: Molecules to Materials*, Wiley-VCH, Weinheim, **2005**.
[31] K. S. Cole, R. H. Cole, *J. Chem. Phys.* **1941**, *9*, 341.
[32] J. Villain, F. Hartmann-Boutron, R. Sessoli, A. Rettori, *Europhys. Lett.* **1994**, *27*, 159.
[33] A. Abragam, B. Bleaney, *Electron Paramagnetic Resonance of Transition Ions*, Dover, New York, **1986**.
[34] S. Ueki, M. Sahlan, T. Ishida, T. Ishida, T. Nogami, *Synth. Met.* **2005**, *154*, 217.
[35] R. L. Carlin, *Magnetochemistry*, Springer, New York, **1986**.

[36] S. Accorsi, A.-L. Barra, A. Caneschi, G. Chastanet, A. Cornia, A. C. Fabretti, D. Gatteschi, C. Mortalo, E. Olivieri, F. Parenti, P. Rosa, R. Sessoli, L. Sorace, W. Wernsdorfer, L. Zobbi, *J. Am. Chem. Soc.* **2006**, *128*, 4742.

[37] a) A. Caneschi, D. Gatteschi, N. Lalioti, C. Sangregorio, R. Sessoli, G. Venturi, A. Vindigni, A. Rettori, M. G. Pini, M. A. Novak, *Angew. Chem.* **2001**, *113*, 1810; *Angew. Chem. Int. Ed.* **2001**, *40*, 1760; b) A. Caneschi, D. Gatteschi, N. Lalioti, C. Sangregorio, R. Sessoli, G. Venturi, A. Vindigni, A. Rettori, M. G. Pini, M. A. Novak, *Europhys. Lett.* **2002**, *58*, 771.

[38] CrysAlis CDD and CrysAlis RED version p171.29.2, Oxford diffraction, Oxfordshire (Great Britain), **2000**.

[39] G. M. Sheldrick, SHELXL-97, Program for refinement of crystal structures, University of Göttingen, Germany, **1997**.

[40] S. Midollini, A. Orlandini, P. Rosa, L. Sorace, *Inorg. Chem.* **2005**, *44*, 2060.

Received: August 16, 2006
Published online: November 30, 2006

